



HAL
open science

Clustering and Turbophoresis in a Shear Flow without Walls

Filippo de Lillo, Massimo Cencini, Stefano Musacchio, Guido Boffetta

► **To cite this version:**

Filippo de Lillo, Massimo Cencini, Stefano Musacchio, Guido Boffetta. Clustering and Turbophoresis in a Shear Flow without Walls. 2016. hal-01279583

HAL Id: hal-01279583

<https://hal.science/hal-01279583>

Preprint submitted on 26 Feb 2016

HAL is a multi-disciplinary open access archive for the deposit and dissemination of scientific research documents, whether they are published or not. The documents may come from teaching and research institutions in France or abroad, or from public or private research centers.

L'archive ouverte pluridisciplinaire **HAL**, est destinée au dépôt et à la diffusion de documents scientifiques de niveau recherche, publiés ou non, émanant des établissements d'enseignement et de recherche français ou étrangers, des laboratoires publics ou privés.

Clustering and Turbophoresis in a Shear Flow without Walls

Filippo De Lillo,^{1, a)} Massimo Cencini,² Stefano Musacchio,³ and Guido Boffetta¹

¹⁾*Dipartimento di Fisica and INFN, Università di Torino, via P. Giuria 1, 10125 Torino, Italy*

²⁾*Istituto dei Sistemi Complessi, Consiglio Nazionale delle Ricerche, via dei Taurini 19, 00185 Rome, Italy*

³⁾*Université Nice Sophia Antipolis, CNRS, Laboratoire J. A. Dieudonné, UMR 7351, 06100 Nice, France*

We investigate the spatial distribution of inertial particles suspended in the bulk of a turbulent inhomogeneous flow. By means of direct numerical simulations of particle trajectories transported by the turbulent Kolmogorov flow, we study large and small scale mechanisms inducing inhomogeneities in the distribution of heavy particles. We discuss turbophoresis both for large and weak inertia, providing heuristic arguments for the functional form of the particle density profile. In particular, we argue and numerically confirm that the turbophoretic effect is maximal for particles of intermediate inertia. Our results indicate that small-scale fractal clustering and turbophoresis peak in different ranges in the particles' Stokes number and the separation of the two peaks increases with the flow's Reynolds number.

PACS numbers: 47.27.-i, 05.45.-a

^{a)}corresponding author:delillo@to.infn.it

I. INTRODUCTION

Turbulent aerosols, dilute solutions of solid particles transported by turbulent flows, are important to the environment and to industry. From combustion processes in coal fire burners, to the dynamics of droplets in clouds, turbulent aerosols impact on our life and the earth's climate^{1,2}. One general feature of turbulent aerosols is their ‘unmixing’ while transported by the flow, which is relevant to several processes including: warm-rain initiation^{3,4}, planetesimal formation in the early solar system⁵⁻⁷, chemical reactions and industrial processes^{8,9}. In recent years much attention has been gathered by the dissipative dynamics resulting from particle inertia which can induce small-scale fractal clustering also in homogeneous flows^{3,4,10-13}. This can have relevant consequences for the rate of collision, coalescence and reaction of particles. Another well known unmixing mechanism in turbulent aerosols is turbophoresis: inertial particles migrating in regions of lower turbulent diffusivity, similarly to thermophoresis¹⁴, for which Brownian particles are subject to an effective drift opposite temperature gradients. Turbophoresis has been mostly studied in presence of boundaries, because as a mechanism for particle deposition in turbulent boundary layers^{15,16} it finds applications both for industrial processes (for removing submicron sized particles from gas streams) and the environment (dry deposition in the atmosphere¹⁷). Nonetheless, the mechanism of turbophoresis is independent of the presence of boundaries as, in principle, it only requires the presence of inhomogeneities in the flow.

In this work we investigate the phenomenology of turbophoresis in a turbulent shear flow without walls. We point out the differences between this mechanism which causes inhomogeneity at large scales and the small-scale clustering which occurs at viscous scales.

II. EQUATIONS OF MOTION AND PARAMETERS

As a paradigmatic case of inhomogeneous unbounded flow, we consider the turbulent Kolmogorov flow, obtained by sustaining the Navier-Stokes equations for the incompressible velocity field \mathbf{u} ,

$$\partial_t \mathbf{u} + \mathbf{u} \cdot \nabla \mathbf{u} = -\nabla p + \nu \Delta \mathbf{u} + \mathbf{F}(z), \quad (1)$$

with a sinusoidal force $\mathbf{F}(z) = F_0 \cos(z/L) \hat{\mathbf{e}}_1$, where p is the pressure, ν the fluid kinematic viscosity, and $\hat{\mathbf{e}}_1$ denotes the unit vector along the horizontal direction. The laminar fixed

point ($\mathbf{u} = U \cos(z/L)\hat{\mathbf{e}}_1$, with $U = L^2 F_0/\nu$) becomes unstable above a critical Reynolds number¹⁸, $Re = UL/\nu > \sqrt{2}$, and the flow eventually becomes turbulent for large Re ¹⁹. A remarkable peculiarity of monochromatic forcing is that the resulting mean velocity profile, $\langle \mathbf{u} \rangle = U \cos(z/L)\hat{\mathbf{e}}_1$, is monochromatic also in the turbulent regimes^{19,20}. Above and in the following, the brackets $\langle \dots \rangle$ denote the average over (x, y) and over time, while $\bar{f} \equiv \int_0^{2\pi L} \langle f \rangle dz / (2\pi L)$. Due to the change of direction of the mean flow every half wavelength, the Kolmogorov flow can be seen as an array of virtual channels flowing in alternate directions without being confined by material boundaries.

The dynamics of a small spherical particle is described by the Maxey-Riley equation²¹. Here, we focus on dilute suspensions of very small particles much heavier than the fluid, whose dynamics is dominated by the Stokes drag. In this limit, the equations for the position \mathbf{x} and velocity \mathbf{v} of each particle simplify to

$$\dot{\mathbf{x}} = \mathbf{v} \tag{2}$$

$$\dot{\mathbf{v}} = -\frac{1}{\tau}[\mathbf{v} - \mathbf{u}(\mathbf{x}, t)] \tag{3}$$

where $\tau = (2a^2\rho_p)/(9\nu\rho)$ is the Stokes time, a and ρ_p are the particle radius and density, respectively while ρ denotes the fluid density. Eqs. (2-3) assumes a Stokes flow around the particle, implying that the particle's Reynolds number must be very small: $Re_p = |\mathbf{v} - \mathbf{u}|a/\nu \ll 1$.

Particle inertia is commonly parametrized in terms of the Stokes number $St = \tau/\tau_\eta$ based on the Kolmogorov time τ_η , i.e., the smallest characteristic time of a turbulent flow. However, turbophoretic effects are expected to be determined by large-scale features of the flow, namely by the interplay between the advection and the inhomogeneities of the eddy diffusivity²². We therefore introduce a particle inertia parameter $S = \tau/T$ by normalizing the particle response time τ with the large-scale eddy turnover time $T = E/\epsilon$, defined as the ratio between the mean kinetic energy E and the energy dissipation rate ϵ . The parameter S is the analogous of $\tau_+ = \tau u^{*2}/\nu$, which is used in wall-bounded flows to parametrize turbophoresis^{23,24} in terms of the friction velocity u^* . This amounts to measuring times in wall units, which control the scaling of inhomogeneities across the wall region.

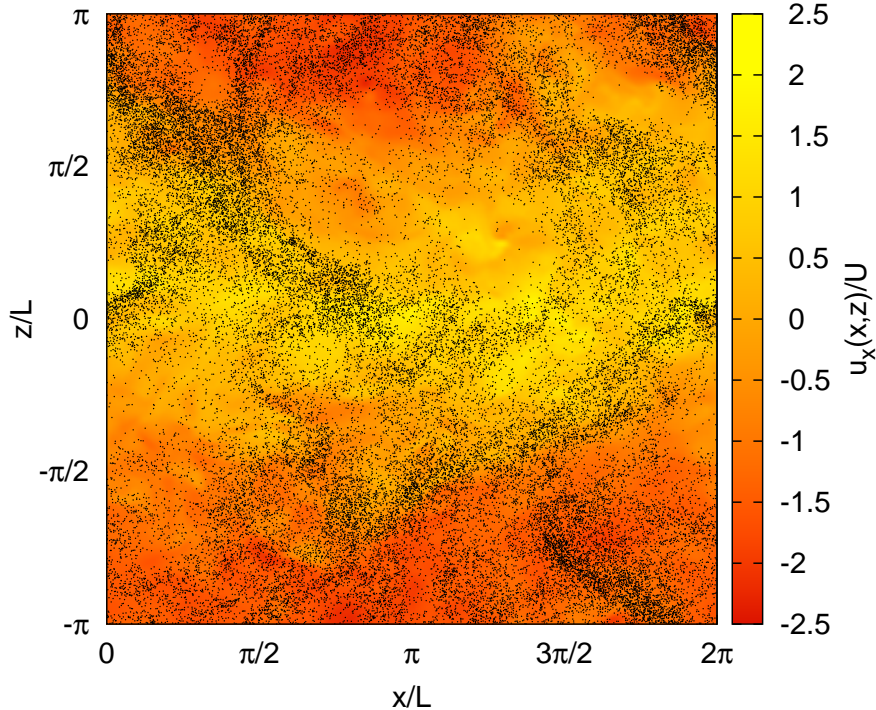


FIG. 1. Particle distribution in a slab of thickness $2\pi L/10$, plotted over the corresponding stream-wise component of velocity (color map, red to yellow online). Particles inertia is $S = 7.9 \times 10^{-2}$ and $Re = 990$.

III. RESULTS AND DISCUSSION

A. Numerical Simulations

We performed direct numerical simulations (DNS) of Eq. (1) by means of a standard pseudospectral code with triple-periodic boundary conditions in a cubic domain of side $L_x = L_y = L_z = 2\pi$ at resolution N^3 , with $N = 128$ and 256 . For each class of particles with given inertia S , we integrated $4 \cdot 10^5$ trajectories according to Eqs. (2-3), with the fluid velocity obtained by linear interpolation from grid nodes to particle positions. Eulerian and Lagrangian dynamics is integrated via a second-order Runge-Kutta scheme. DNS parameters are reported in Table I.

Large-scale inhomogeneities are clearly visible in the particle distribution in Fig. 1. To reveal the correlations of particle positions with the shear-normal structure of the flow it is necessary to consider statistically averaged quantities. Figure 2 shows typical fluid velocity and particle number-density profiles obtained by averaging over the x and y directions

| N | ν | L | F | U | T | ϵ | Re |
|-----|--------------------|-----|-----------------------|------|------|-----------------------|------|
| 128 | 1×10^{-3} | 1.0 | 8×10^{-3} | 0.23 | 36.3 | 9.31×10^{-4} | 230 |
| 256 | 1×10^{-3} | 1.0 | 1.28×10^{-1} | 0.99 | 9.36 | 6.41×10^{-2} | 990 |

TABLE I. DNS parameters: N resolution, ν kinematic viscosity, L forcing scale, F forcing amplitude, U amplitude of mean velocity profile, T large-scale time, ϵ energy dissipation rate, Reynolds number $Re = UL/\nu$.

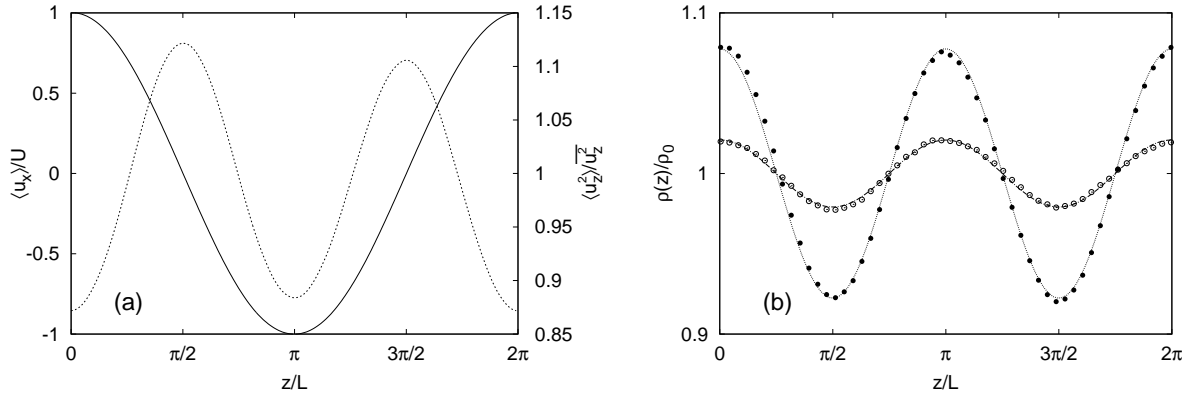


FIG. 2. Fluid velocity and particle distribution profiles at $Re = 990$. (a) profiles of the longitudinal velocity $\langle u_x \rangle$ (solid line, left axis) and the fluctuations in shear-normal kinetic energy $\langle u_z^2 \rangle$ (dashed line, right axis) of the flow. The small asymmetry in $\langle u_z^2 \rangle$ is due to the finite statistics. (b) particle number density profiles $\rho(z)$ for $S = 7.9 \times 10^{-2}$ (filled circles) and $S = 2.6 \times 10^{-3}$ (empty circles), compared with the functional form (4) (lines, fitted).

(normal to the shear) and over very long integration of hundreds of large-eddy-turn-over-times. The modulation of the density profiles closely reflects the structure of the mean flow: particles concentrate in the regions of maximal mean flow and minimal mean shear, away from the maxima of turbulent energy.

As it is shown in (Fig. 2), the particle density profiles are accurately fitted by:

$$\rho(z) = \rho_0(1 + a(S) \cos(2z/L)) \quad (4)$$

where $\rho_0 = 1/L_z$ is the mean uniform density and the only free-parameter is $a(S)$, which accounts for the dependence on the particles' inertia. In the following we discuss a heuristic argument which gives support to the empirical formula (4).

B. Turbophoresis

A common approach to derive theoretical predictions for the dynamics of inertial particles is by modeling the velocity field as a Gaussian, short-correlated noise¹⁰. With this assumption, one can write²² a Fokker-Planck equation for the probability density $P(z, v)$ to find a particle in z with vertical velocity v , in which turbulence is parametrized by a space-dependent eddy diffusivity $\kappa(z)$ acting on velocity and derived from Eq. (3). It is then possible, in the limit of fast relaxation of the velocity distribution^{17,22}, to obtain an equation for the marginal distribution $\rho(z) = \int dv P(z, v)$, which reads $\partial_t \rho(z) = \partial_z J(z)$, where the flux is $J(z) = \partial_z [\kappa(z) \rho]$. For the fluxless steady state one obtains the prediction $\rho \sim \kappa^{-1}(z)$ which, in analogy with thermophoresis²⁵, implies that particles concentrate in the minima of diffusivity. This behaviour is substantially different from that of a classical, passively advected scalar field θ , where the eddy-diffusivity would appear in the flux in the Fickian form $J = \kappa(z) \partial_z \theta$, leading to a homogeneous steady state. Standard dimensional arguments suggest that the eddy diffusivity is proportional to the mean square velocity $\kappa(z) \propto \tau_c \langle u_z^2 \rangle$ (with τ_c an appropriate correlation time), so that the above result implies $\rho(z) \propto \langle u_z^2 \rangle^{-1}$. In the case of the Kolmogorov flow, the profile of the mean square vertical velocity is found to be $\langle u_z^2 \rangle \propto U^2(1 - b \cos(2z/L))$, with $b \ll 1$ and weakly depending on Re^{20} . Using a first-order Taylor expansion in b one recovers the expression (4). It is worth remarking that the above argument relies on two assumptions. First, the correlation time of the flow is set to zero. Second, the particle Stokes time τ is assumed to be small enough to justify the fast relaxation of the velocity distribution. In this limit the amplitude of the spatial modulation of the particle density profile would not depend on S , namely $a(S) = b$. The latter, quantitative prediction does not hold if the flow has a finite correlation time, as in our case. However, we find that Eq. (4) gives the correct shape for the density profile for particles with Stokes times both shorter and longer than the correlation time of the flow, provided that the amplitude $a(S)$ is allowed to depend on inertia.

The analogy with thermophoresis can be exploited for particles with large inertia. In this limit, the particles can be seen as a gas in equilibrium with the turbulent environment and we can interpret the spatial variations of the mean particle vertical velocity variance, $\langle v_z^2(z) \rangle$, as the analogous of a space-dependent temperature field¹⁷. Assuming the local diffusivity proportional to the temperature, i.e. $\kappa(z) \sim \langle v_z^2(z) \rangle$, the particle density profile is therefore

expected to be $\rho(z) \propto \langle v_z^2 \rangle^{-1}$, which is in fairly good agreement with numerical results for large S (see Fig. 3). Moreover, we find that the particle velocity profile $\langle v_z^2 \rangle$ has the same spatial dependence as the fluid one $\langle u_z^2 \rangle$, but the amplitude of the spatial modulation decreases at increasing inertia. This leads to the prediction that the amplitude $a(S)$ in (4) is a decreasing function of the inertia for large S .

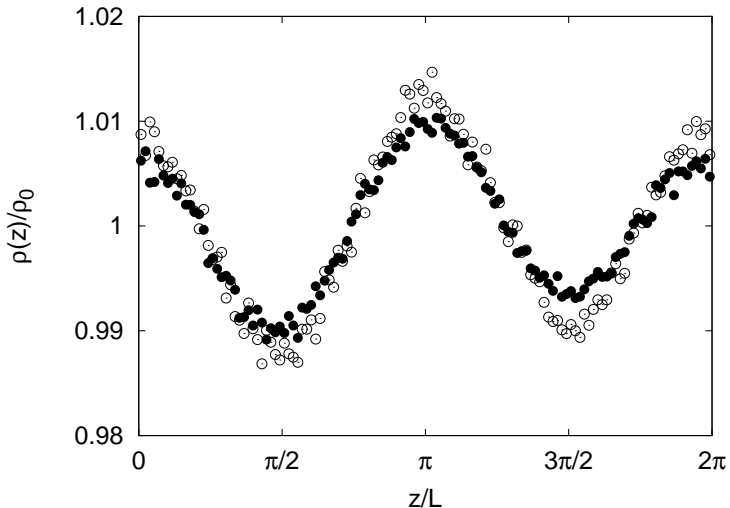


FIG. 3. Particle number density profiles $\rho(z)$ for $S = 4.1$ (filled circles) at $\text{Re} = 230$. The particle distribution is compared the prediction $\rho(z)/\rho_0 = \langle v_z^2 \rangle^{-1} L_z / \int_0^{L_z} \langle v_z^2 \rangle^{-1} dz$ (empty circles). Statistical fluctuations are due to the slow convergence observed for large S .

The scenario is different for particles whose Stokes time is of the order of the eddy-turn-over times in the inertial range of turbulence. Such particles are able to follow only turbulent eddies of size ℓ with a turn-over time, τ_ℓ , longer than their Stokes time, i.e. $\tau_\ell > \tau$. Smaller eddies still act as a colored noise giving raise to a space-dependent effective diffusivity responsible for turbophoresis. Conversely, eddies with $\tau_\ell > \tau$ mix the particles almost like tracers, thus reducing the turbophoretic accumulation. Turbophoretic unmixing is therefore enhanced as S increases, because a larger fraction of eddies contribute to it. Assuming that the profile of the effective diffusivity due to the small eddies has a monochromatic modulation one recovers the prediction (4) in which $a(S)$ increases with S for small values of S . Hence, we expect that $a(S)$ attains its maximum when the particle response time is of the same order of the characteristic time of the large-scale structures of the flow ($S \simeq O(1)$).

At the heart of the arguments discussed above, there is the notion that turbophoresis

drives particles away from the maxima of turbulent energy, which correspond to maxima of the eddy diffusivity. In the case of the Kolmogorov flow, the maxima of turbulent fluctuations occur where the shear of the mean flow is maximum and the mean flow vanishes, i.e., at the borders between the virtual channels. Therefore, particles are driven toward the center of the virtual channels. This is in contrast with the case of a turbulent channel (or pipe) flow, in which turbulence is intense in the bulk and vanishes in the viscous sub-layer close to the walls. In this case turbophoresis drives the particles away from the bulk and concentrates them along the walls²⁶⁻²⁸. In this sense, the fact that turbophoresis may eventually accumulate the particles to regions of large or small mean velocity (or mean shear) is an incidental (albeit relevant for applications) consequence of the details of the particular flow considered.

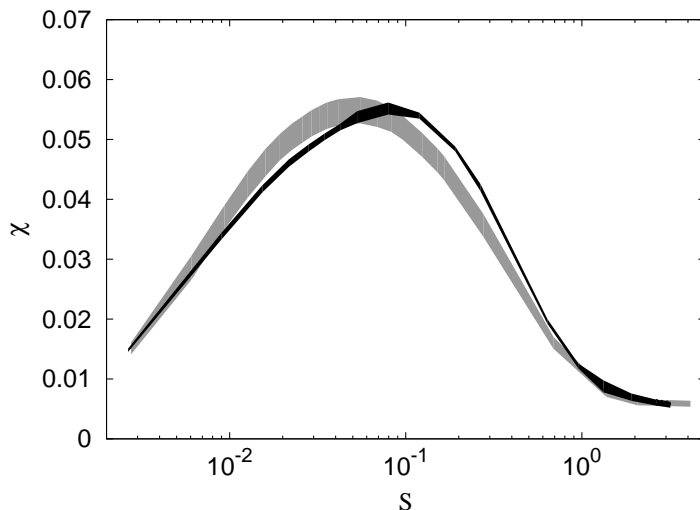


FIG. 4. Rms relative deviation χ from the homogeneous distribution plotted as a function of S for $Re = 230$ (grey curve) and $Re = 990$ (black curve). The thickness of the curves reflects the statistical fluctuations around the mean value.

The overall effect of turbophoresis can be quantified by means of the rms relative deviation of the mean density profile $\rho(z)$ from the uniform distribution ρ_0 as $\chi = [1/L_z \int_0^{L_z} (1 - \rho(z)/\rho_0)^2 dz]^{1/2}$. For the specific profile (4), clearly we have $\chi(S) = a(S)/\sqrt{2}$. This quantity is plotted in Fig.4 as a function of the inertia parameter. In agreement with expectations, the turbophoretic effect is not monotonic as a function of inertia. It displays a maximum at $S \simeq 10^{-1}$. The shape of the curves is not strongly affected by changing Re even though we observe, within the statistical uncertainties, a weak dependence of the position of the maximum.

Remarkably, deviations from the uniform distribution are present also for particles whose Stokes time is much smaller than the Kolmogorov time. Arguments based on local variations of the eddy diffusivity can not be used to explain the origin of such inhomogeneities, because the particle relaxation time is shorter than the shortest eddy-turnover time of the flow. The mechanism responsible for such inhomogeneities also for $St \ll 1$ is related to the weak compressibility of the particle velocity field. When $St \ll 1$, expanding at first order in τ the velocity of the particle one has $\mathbf{v} = \mathbf{u} - \tau (\partial_t \mathbf{u} + \mathbf{u} \cdot \nabla \mathbf{u}) + o(\tau)$ (see e.g. Ref.¹⁰). The mean vertical profile of the divergence of the particle velocity field is $\langle \nabla \cdot \mathbf{v} \rangle = -\tau \langle \nabla \cdot (\mathbf{u} \cdot \nabla \mathbf{u}) \rangle = -\tau \partial_z^2 \langle u_z^2 \rangle$. The mean divergence is positive in the maxima of $\langle u_z^2 \rangle$ and is negative in the minima, providing an explanation for the accumulation of inertial particles in the minima of $\langle u_z^2 \rangle$, observed at very weak inertia.

C. Small-Scale Clustering

Besides the large-scale effects discussed above, inertial particles transported in a turbulent flow display small-scale clustering. Small-scale spatial inhomogeneities originate from the dissipative dynamics in the 6-dimensional position-velocity phase space (\mathbf{x}, \mathbf{v}) ^{10,11}. In particular, inertial particle motion asymptotically takes place on a (multi-)fractal set in phase space. A fractal dimension smaller than space dimension signals an enhanced probability to find particle pairs at short separation. Indeed, the probability to find particle pairs at separation below a certain r (smaller than the Kolmogorov scale) grows as r^{D_2} , with $D_2 = 3$ for uniformly distributed particles in three dimensions²⁹. The correlation dimension D_2 is thus commonly used as a measure of clustering. In Fig. 5 we plot the co-dimension $3 - D_2$ as a function of $St = \tau/\tau_\eta$ for two values of Re . In agreement with previous results obtained in homogeneous, isotropic turbulence (HIT)¹³, we find that the fractal co-dimension has only a very weak dependence on Re . Moreover, we find that it is not affected by the large-scales inhomogeneities of the Kolmogorov flow³⁰ as apparent from Fig. 5 where published data for D_2 of heavy particles from a HIT simulation¹³ are shown for comparison³¹. On the contrary, the turbophoretic clustering measured by χ plotted as a function of St has a strong dependence on Re : the maximum is attained for larger St as Re increases (see Fig.5).

The different Re -dependence of the two phenomena reflects their different nature. The small-scale clustering is due to the chaotic dynamics at viscous scales, therefore it is most

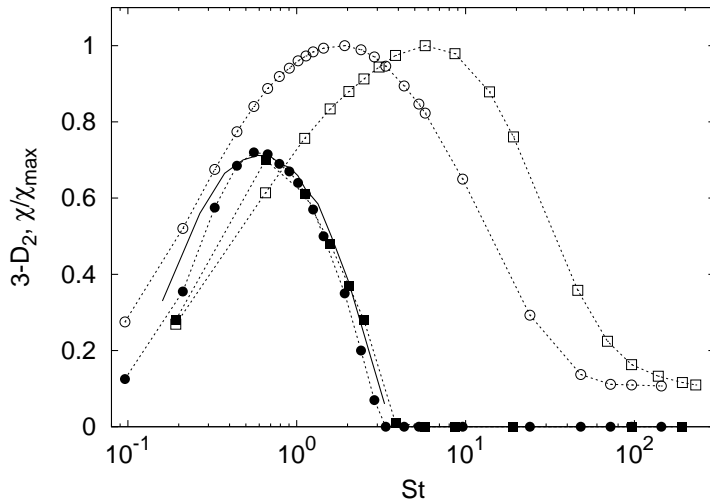


FIG. 5. Correlation co-dimension $3 - D_2$ of particle distributions (filled symbols) and rms relative deviation from uniform distribution χ (empty symbols, same data of Fig. 4) as a function of St (filled symbols) and for $Re = 230$ (circles) and $Re = 990$ (squares). The continuous line show the comparison with the D_2 computed for a HIT case from¹³ at $Re_\lambda = 185$.

effective at $St \sim O(1)$, i.e. when $\tau \simeq \tau_\eta$. Conversely, turbophoresis is the result of the transport of particles across the large-scale inhomogeneities of the flow. Its effects is maximum for particles with response time of the order of the large-scale eddy turnover time T , i.e., at $S \simeq 1$. As the Reynolds number grows, the scale separation between the two unmixing mechanisms is expected to grow as $T/\tau_\eta \sim Re^{1/2}$, as shown in Fig. 5.

IV. CONCLUSIONS

We have investigated the phenomenon of turbophoresis and fractal clustering of heavy inertial particles in the bulk of inhomogeneous flow, by performing DNS of the dynamics of heavy particles transported by the turbulent Kolmogorov flow. The emerging scenario in the limit of large Re is the following. The distribution of particles with small inertia is characterized by a strong fractal clustering at small scales, but is weakly affected by turbophoresis. On the contrary, particles with large inertia experience strong turbophoretic accumulation at large scales while remaining uniformly distributed at small scales. The turbophoretic effect is maximum for particles with Stokes time of the order of the large-scale eddy-turnover times of the turbulent flow. Conversely, small-scale fractal clustering is

maximal for particles with Stokes times comparable with the Kolmogorov time.

Turbophoresis is characterized by large scale particle density profiles which are strongly correlated to the inhomogeneities of the flow. In particular, particle density is maximal in the minima of the turbulent eddy diffusivity, which for the case of the Kolmogorov flow coincides with the maxima of the mean flow. This is an important difference with what observed in wall bounded flows, where turbophoresis concentrates particles in regions of minimum mean flow close to the boundaries and demonstrates that the regions of particle accumulation depend on the details of the flow.

ACKNOWLEDGMENTS

We acknowledge support from the European COST Action MP1305 “Flowing Matter”. Numerical simulations were performed at CINECA via the INFN-FieldTurb grant.

REFERENCES

- ¹G. Hidy, *Aerosols: an industrial and environmental science* (Elsevier, 2012).
- ²M. W. Reeks, “Transport, mixing and agglomeration of particles in turbulent flows,” *Flow, Turbulence and Combust.* **92**, 3–25 (2014).
- ³G. Falkovich, A. Fouxon, and M. Stepanov, “Acceleration of rain initiation by cloud turbulence,” *Nature* **419**, 151–154 (2002).
- ⁴R. A. Shaw, “Particle-turbulence interactions in atmospheric clouds,” *Annu. Rev. Fluid Mech.* **35**, 183–227 (2003).
- ⁵S. Weidenschilling, “Dust to planetesimals: Settling and coagulation in the solar nebula,” *Icarus* **44**, 172–189 (1980).
- ⁶P. Tanga, A. Babiano, B. Dubrulle, and A. Provenzale, “Forming planetesimals in vortices,” *Icarus* **121**, 158–170 (1996).
- ⁷A. Bracco, P. Chavanis, A. Provenzale, and E. Spiegel, “Particle aggregation in a turbulent keplerian flow,” *Physics of Fluids (1994-present)* **11**, 2280–2287 (1999).
- ⁸J. Williams and R. Crane, “Drop coagulation in cross-over pipe flows of wet steam,” *J. Mech. Eng. Sci.* **21**, 357–360 (1979).

- ⁹Y. Xiong and S. E. Pratsinis, “Gas phase production of particles in reactive turbulent flows,” *J. Aerosol Sci.* **22**, 637–655 (1991).
- ¹⁰E. Balkovsky, G. Falkovich, and A. Fouxon, “Intermittent distribution of inertial particles in turbulent flows,” *Physical Review Letters* **86**, 2790 (2001).
- ¹¹J. Bec, “Fractal clustering of inertial particles in random flows,” *Physics of Fluids* **15**, L81–L84 (2003).
- ¹²K. Duncan, B. Mehlig, S. Östlund, and M. Wilkinson, “Clustering by mixing flows,” *Phys. Rev. Lett.* **95**, 240602 (2005).
- ¹³J. Bec, L. Biferale, M. Cencini, A. Lanotte, S. Musacchio, and F. Toschi, “Heavy particle concentration in turbulence at dissipative and inertial scales,” *Phys. Rev. Lett.* **98**, 084502 (2007).
- ¹⁴J. C. Maxwell, “On stresses in rarefied gases arising from inequalities of temperature.” *Proc. Royal Soc. London* **27**, 304–308 (1878).
- ¹⁵G. Sehmel, “Particle deposition from turbulent air flow,” *J. Geophys. Res.* **75**, 1766–1781 (1970).
- ¹⁶J. W. Brooke, K. Kontomaris, T. Hanratty, and J. B. McLaughlin, “Turbulent deposition and trapping of aerosols at a wall,” *Phys. Fluids A* **4**, 825–834 (1992).
- ¹⁷M. Caporali, F. Tampieri, F. Trombetti, and O. Vittori, “Transfer of particles in non-isotropic air turbulence,” *J. Atmos. Sci.* **32**, 565–568 (1975).
- ¹⁸G. I. Sivashinsky, “Weak turbulence in periodic flows,” *Physica D: Nonlinear Phenomena* **17**, 243–255 (1985).
- ¹⁹V. Borue and S. A. Orszag, “Numerical study of three-dimensional kolmogorov flow at high reynolds numbers,” *J. Fluid Mech.* **306**, 293–323 (1996).
- ²⁰S. Musacchio and G. Boffetta, “Turbulent channel without boundaries: The periodic kolmogorov flow,” *Phys. Rev. E* **89**, 023004 (2014).
- ²¹M. R. Maxey and J. J. Riley, “Equation of motion for a small rigid sphere in a nonuniform flow,” *Phys. Fluids* **26**, 883–889 (1983).
- ²²S. Belan, I. Fouxon, and G. Falkovich, “Localization-delocalization transitions in turbophoresis of inertial particles,” *Phys. Rev. Lett.* **112**, 234502 (2014).
- ²³G. Sardina, P. Schlatter, L. Brandt, F. Picano, and C. Casciola, “Wall accumulation and spatial localization in particle-laden wall flows,” *J. Fluid Mech.* **699**, 50–78 (2012).
- ²⁴C. Marchioli and A. Soldati, “Mechanisms for particle transfer and segregation in a tur-

- bulent boundary layer,” *Journal of fluid Mechanics* **468**, 283–315 (2002).
- ²⁵C. López and U. M. B. Marconi, “Multiple time-scale approach for a system of brownian particles in a nonuniform temperature field,” *Phys. Rev. E* **75**, 021101 (2007).
- ²⁶J. B. McLaughlin, “Aerosol particle deposition in numerically simulated channel flow,” *Phys. Fluids A* **1**, 1211–1224 (1989).
- ²⁷D. Kaftori, G. Hetsroni, and S. Banerjee, “Particle behavior in the turbulent boundary layer. ii. velocity and distribution profiles,” *Physics of Fluids* **7**, 1107–1121 (1995).
- ²⁸G. Sardina, F. Picano, P. Schlatter, L. Brandt, and C. M. Casciola, “Large scale accumulation patterns of inertial particles in wall-bounded turbulent flow,” *Flow, turbulence and combustion* **86**, 519–532 (2011).
- ²⁹G. Paladin and A. Vulpiani, “Anomalous scaling laws in multifractal objects,” *Physics Reports* **156**, 147–225 (1987).
- ³⁰In principle the fractal clustering could depend on z due to the space-dependent fluctuations of the energy dissipation which changes the local value of St . However we did not observe measurable variations of D_2 in the vertical direction, consistently with the results of²⁰ showing variations in ϵ within 10% across the domain.
- ³¹Small-scale clustering can display effects of flow anisotropy³² which we did not investigate.
- ³²P. Gualtieri, F. Picano, and C. Casciola, “Anisotropic clustering of inertial particles in homogeneous shear flow,” *Journal of Fluid Mechanics* **629**, 25–39 (2009).